

Published in final edited form as:

DNA Repair (Amst). 2011 September 5; 10(9): 953–960. doi:10.1016/j.dnarep.2011.07.002.

Guanine repeat-containing sequences confer transcription-dependent instability in an orientation-specific manner in yeast

Nayun Kim^{a,*} and Sue Jinks-Robertson^a

^aDepartment of Molecular Genetics and Microbiology, Duke University Medical Center, Durham NC 27710

Abstract

Non-B DNA structures are a major contributor to the genomic instability associated with repetitive sequences. Immunoglobulin switch Mu ($S\mu$) region sequence is comprised of guanine-rich repeats and has high potential for forming G4 DNA, in which one strand of DNA folds into an array of guanine quartets. Taking advantage of the genetic tractability of *Saccharomyces cerevisiae*, we developed a recombination assay to investigate mechanisms involved in maintaining stability of G-rich repetitive sequence. By embedding $S\mu$ sequence within recombination substrates under the control of a tetracycline-regulatable promoter, we demonstrate that the rate and orientation of transcription both affect the stability of $S\mu$ sequence. In particular, the greatest instability was observed under high-transcription conditions when the $S\mu$ sequence was oriented with the C-rich strand as the transcription template. The effect of transcription orientation was enhanced in the absence of the Type IB topoisomerase Top1, possibly due to enhanced R-loop formation. Loss of Sgs1 helicase and RNase H activity also increased instability, suggesting they may cooperatively function to reduce the formation of non-B DNA structures in highly transcribed regions. Finally, the $S\mu$ sequence was unstable when transcription elongation was perturbed due to a defective THO complex. In a THO-deficient background, there was further exacerbation of orientation-dependent instability associated with the ectopically expressed, single-strand cytosine deaminase AID. The implications of our findings to understanding instability associated with potential G4 DNA forming sequences are discussed.

Keywords

G4 DNA; R-loops; genome instability; transcription; recombination

1. Introduction

Repetitive sequences that can adopt non-B structures *in vivo* are associated with increased genetic instability [1, 2]. Non-B DNA structures include triplex or H-DNA formed by polypurine tracts (for example, GAA triplet repeats), cruciforms formed by inverted repeats, and left-handed Z-DNA formed by alternating purines and pyrimidines. G-quartets,

© 2011 Elsevier B.V. All rights reserved.

*Corresponding author. Tel: 1 919 684 0042 Fax: 1 919 684 2790 nayun.kim@duke.edu, Address: 213 Research Drive CARL #384 Box 3020 Durham, NC 27710.

Publisher's Disclaimer: This is a PDF file of an unedited manuscript that has been accepted for publication. As a service to our customers we are providing this early version of the manuscript. The manuscript will undergo copyediting, typesetting, and review of the resulting proof before it is published in its final citable form. Please note that during the production process errors may be discovered which could affect the content, and all legal disclaimers that apply to the journal pertain.

Conflict of interest statement

The authors declare that we have no conflict of interest.

comprised of four guanines assembled into a planar configuration through Hoogsteen bonding [3], are also an example of a non-B structure forming sequence motifs. When DNA contains more than four tracts of at least three guanines, it can form a higher order structure called G4 DNA, which consists of multiple G-quartets stabilized by stacking on top of each other [4]. Sequences with potential for G4 DNA formation are found throughout the genomes of bacteria, yeast and higher eukaryotes. Notably, telomeres, rDNA loci, immunoglobulin heavy-chain switch regions, and G-rich minisatellites have high potential to form G4 DNA [4, 5]. G4 DNA forming potential also correlates with genomic regions that are relatively unstable, such as proto-oncogenes and sites of frequent translocation breakpoints [6]. In particular, chromosomal translocations involving G-rich immunoglobulin switch regions have been observed in various cancer cell lines [7].

G4 DNA formation requires exposure of the G-rich strand as a single strand, as would occur during transcription, DNA repair or lagging-strand replication. In the case of transcription, the limited single-stranded character of a non-transcribed, G-rich strand can be further enhanced by the relatively stable base pairing between the corresponding deoxyribocytosine (dC)-rich template and riboguanine (rG)-rich transcript. The higher-order DNA structure involving G4 DNA on one strand and an extended RNA:DNA hybrid on the other is referred to as a G-loop [4]. Consistent with a role for RNA:DNA hybrids in G4 DNA formation, disruption of the strong base pairing between rG and dC by substituting ribo-inosine for rG has been shown to reduce G-loop structures *in vitro* [8]. Although recent reports clearly show that the G-rich sequences of immunoglobulin class switch regions and telomeres can assume G-loop structures *in vitro* and in bacterial cells [8], the biological significance of such structures is not well understood [5]. Because transcription of the G-rich switch region is required for class-switch recombination (CSR), it has been speculated that co-transcriptionally formed G-loop structures may be relevant to both regulated CSR and to unintended chromosomal breaks and rearrangements [4].

In *E. coli*, formation of G-loop structures requires activated transcription and is inhibited in the presence of the RecQ DNA helicase and RNase H, which degrades the RNA strand of RNA:DNA hybrids [8]. Although individual effects of RecQ and RNase H on G-loop formation were not reported, data are consistent with G4 DNA being directly dissolved by helicase activity and/or its formation inhibited by RNase H. *In vivo*, the human RecQ family DNA helicase BLM, as well as the yeast homolog Sgs1, is important for general genome stability, especially in maintaining the integrity of G-rich regions such as telomeres and rDNA repeats [9-13]. In *in vitro* assays, BLM and Sgs1 have been shown to efficiently unwind G4 DNA [14, 15]. The yeast Pif1 helicase has also been shown to unwind G4 DNA, specifically that formed by the human G-rich minisatellite CEB1 [16]. While CEB1 repeats are very unstable in a *pif1* mutant background, loss of Sgs1 has no effect on the stability of these particular repeats. Finally, the Dog-1 DNA helicase of *C. elegans*, which is an ortholog of mammalian FANCI, stabilizes sequences with high G4-forming potential in this organism [17].

Valuable insight into mechanisms of genomic instability has come through the use of *Saccharomyces cerevisiae* as a model system to examine specific mammalian sequence motifs. Examples include the CAG/CTG repeat involved in Huntington's disease and myotonic dystrophy type 1 [18], the G-rich human minisatellite CEB1 [16], the CGG/CCG repeat involved in fragile X syndrome [19], the GAA/TTC repeat involved in Friedreich's ataxia [20], and the inverted ALU repeats present throughout the human genome [21]. In the current study, we use a recombination assay to analyze whether sequences with high potential to form G4 DNA lead to genomic instability in yeast. Results demonstrate that transcription of the immunoglobulin heavy chain switch Mu ($S\mu$) sequence is associated

with an orientation-dependent increase in recombination in some mutant backgrounds, consistent with the formation of co-transcriptional G-loops.

2. Material and Methods

2.1 Construction of plasmids

pSR886 (*lys2::SμF*) and pSR887 (*lys2::SμR*) were constructed by inserting a 750-bp *Sau3AI* fragment from pT7-Sμ [22] into a unique *BglIII* site within *LYS2* sequences of pSR633 (see Figure 1A and 1B). pSR633 contains a 3.5 kb *XbaI/BamHI lys2Δ3'* fragment in the *URA3*-integrating vector pRS306 [23]. pSR953 (*lys2::cβ2*) was constructed by inserting an 800-bp *BglIII/BamHI* chicken β-globin 2 cDNA (*Cβ2*) fragment into the *BglIII* site of a plasmid containing the previously described *lys2-oligo* allele [24]. pSR877 (pRS402-*lys2Δ3'*) was constructed by inserting a 1.3 kb *NotI/SpeI* fragment of *LYS2* gene into *NotI/SpeI*-digested pRS402, an *ADE2* integrating vector [25].

The plasmid pESC-LEU-hAIDSc [26] was constructed by cloning the human AID gene (hAID) engineered to contain favored yeast codons into *BamHI/SalI*-digested pESC-LEU (Stratagene) and was a gift from Y. Pavlov (University of Nebraska). To replace the *LEU2* maker with a *Hyg^R* gene, pESC-LEU and pESC-LEU-hAIDSc were digested with *EcoRV* and *BglIII* and ligated to a 1.3 kb *EcoRV/BglIII* fragment from the plasmid hphMX4 [27].

2.2 Construction of yeast strains

All yeast strains were derived from YPH45 (*MATa ura3-52 ade2-101_{oc} trp1Δ1*). Construction of a strain with the *pTET-LYS2* gene positioned at the *HIS4* locus near *ARS306* on chromosome III was previously described [28]. The *LYS2* wild-type allele placed in opposite orientation relative to *ARS306* was replaced with the *lys2::SμF*, *lys2::SμR*, or *lys2::Cβ2* allele by standard two-step allele replacement (Figure 1C). pSR877 was digested with *StuI* to target insertion of the *lys2Δ3'* allele to the *ADE2* locus on chromosome XV; integration of a single copy of pSR877 was confirmed by PCR.

Mutant strains were constructed by one-step gene disruption using PCR-generated deletion cassettes; primers are available upon request. As appropriate, the *loxP*-flanked *URA3KI* or *TRP1* marker was deleted following transformation with a Cre recombinase-expressing plasmid [29]. For some strains, the *Hyg^R* gene originally used to select for deletion of the endogenous *LYS2* locus was replaced with the *Nat^R* gene using *NotI*-digested pAG25 [27].

2.3. Recombination rates

Fluctuation analysis was carried out at 30°C using at least two independent isolates of each strain. First, 4-5 colonies were used to inoculate 5 ml of non-selective YEP medium (1% yeast extract, 2% Bacto-peptone, 250 mg/l adenine; 2% agar for plates) supplemented with 2% glycerol plus 2% ethanol (YEPGE). As appropriate, the liquid medium was supplemented with doxycycline hyclate (DOX; obtained from Sigma) to 2000 ng/ml. Following overnight growth, cells were diluted to approximately 250,000 cells/ml in the same liquid medium and six 1-ml aliquots were transferred to separate tubes. Following 3 additional days of growth, appropriately diluted cells were plated on SD-Lys plates to select for recombinants or on YPD to determine the total number of cells in each culture. Colonies were counted after 2 days. Recombination rates were determined using the method of median and 95% confidence intervals were calculated as described previously [30]. 12 to 20 cultures were used for each rate determination.

For the measurement of the hAID-induced recombination rates, two independent isolates of each strain were transformed with pESC-HYG (pSR926) or pESC-HYG-hAIDSc (pSR927).

Following selection of transformants on YPD plates supplemented with 0.3 g/l hygromycin B (Invitrogen), 4-5 colonies were used to inoculate a 5 ml overnight culture. The remainder of the fluctuation procedure was as described above, except that YEP liquid media was supplemented with 0.3 g/l hygromycin B, 2 % galactose, 2 % glycerol and 2 % ethanol.

3. Results

3.1. A system for examining effects of switch region sequence on recombination

We chose the immunoglobulin switch region as a model example of a sequence with the potential to form G-loops during transcription [3, 8]. Switch region sequences are required for heavy chain CSR and contain degenerate G-rich repeats of several kb in length [31]. To examine associated instability, we used a 770-bp fragment of the mouse switch mu ($S\mu$) core sequence containing 20 copies of the repeat (GAGCT)_nGGGGT plus additional degenerate repeats (Pubmed Accession #J00442 - Figure 1A). This fragment was inserted in both orientations within a doxycycline (DOX)-repressible *pTET-LYS2* gene on chromosome III of a haploid yeast strain. In this system, transcription is activated by tetR-VP16 binding to *tetO* sequence in absence of DOX and repressed by the tetR'-Ssn6 repressor protein binding to *tetO* in the presence of DOX [32]. We previously showed that 1000 ng/ml DOX in the growth medium reduced the transcription of the *pTET-LYS2* gene by approximately 1000-fold [28]. In the *pTET-lys2::S μ F* "forward" construct, the G-rich sequence is on the top, non-transcribed strand and thus mimics the physiological orientation. In the *pTET-lys2::S μ R* "reverse" construct, the $S\mu$ fragment is in the inverse orientation, resulting in the C-rich sequence being on the top strand (Figure 1B). Because G-loop formation has been shown to occur only when the non-transcribed strand contains the G-rich sequence [8], G-loops have the potential to form when the $S\mu$ F construct is highly transcribed but not when the $S\mu$ R construct is highly transcribed.

As a control allele with no G4-forming potential, an 800 bp fragment of chicken β -globin 2 cDNA was inserted into the *pTET-LYS2* gene (*pTET-lys2::C β 2* allele). The GC content of this sequence (63%) is similar to that of the $S\mu$ sequence inserted to generate the *pTET-lys2::S μ* alleles (62%), but this sequence has no biased distribution of G's and C's between the two strands. The $C\beta$ 2 sequence contains only four widely separated runs of G's and six runs of C's greater than 4 nt, and is not expected to form G4 DNA or G-loops when transcribed. Finally, to provide a donor sequence for the repair of broken or gapped *pTET-lys2* reporter alleles by homologous recombination, a *lys2* allele with a 3' deletion and under control of its native promoter (*pLYS-lys2 Δ 3'* allele) was inserted into the *ADE2* locus on chromosome XV. It should be noted that, because the *pTET-lys2* and *pLYS-lys2 Δ 3'* alleles are in different orientations relative to their respective centromeres, crossover products are inviable (Figure 1C). The systems used here thus measure only rates of noncrossover recombinants.

3.2. Loss of RNase H activity affects $S\mu$ F- more than $S\mu$ R-associated recombination

The RNase H class of enzyme degrades the RNA strand of RNA:DNA hybrids, thus promoting the reannealing of the two strands of DNA during transcription. Because formation of a stable RNA:DNA hybrid is a central feature of the G-loop structure, RNase H activity is predicted to limit the formation and/or stability of G-loops. In yeast, three RNase H enzymes have been identified [33]. RNase H1 is a single subunit enzyme encoded by *RNH1* gene. RNase H2 is composed of three subunits, with the *RNH201* gene (also referred to as *RNH35* or *RNH2A*) encoding the highly conserved catalytic subunit. Finally, RNase H70 was identified based on amino acid homology, but RNase H activity has not been confirmed. Because RNase H1 and RNase H2 appear to have redundant roles in removing RNA:DNA hybrids in yeast [34, 35], we deleted both the *RNH1* and *RNH201* genes in

strains containing the *pTET-lys2::SμF*, *pTET-lys2::SμR* or *pTET-lys2::Cβ2* construct in order to study the effect of RNase H deficiency on recombination.

Under low-transcription conditions (+DOX) in a wild-type (WT) background, the recombination rate for the *pTET-lys2::SμF* and *pTET-lys2::SμR* alleles was indistinguishable, and was approximately 3-fold higher than the recombination rate obtained with the control *pTET-lys2::Cβ2* construct (Table 1). RNase H deficiency under low-transcription conditions was associated with a small (~2 fold) elevation in the recombination rates for the *pTET-lys2::SμF* and *pTET-lys2::SμR* constructs, and a somewhat larger increase (~10-fold) for the *Cβ2* construct. Under high transcription conditions in a WT background, the recombination rates of *pTET-lys2::SμF*, *pTET-lys2::SμR* and *pTET-lys2::Cβ2* constructs were elevated to similar extents (6.9, 4.6-fold and 3.1, respectively). When transcription was activated in the RNase H-deficient strains, however, the rate of recombination was elevated 87-fold for the *pTET-lys2::SμF* construct but only 16-fold for the *pTET-lys2::SμR* and *pTET-lys2::Cβ2* constructs. Under high-transcription conditions in the RNase H-deficient background, the recombination rate associated with the *pTET-lys2::SμF* allele was 5.4- and 3.4-fold greater than that obtained with the *pTET-lys2::SμR* and *pTET-lys2::Cβ2* constructs, respectively.

3.3. Effect of Sgs1 loss on SμF-, SμR- and Cβ2-associated recombination

Sgs1 is the only member of RecQ DNA helicase family present in yeast, and we examined its effect on stability of the *pTET-lys2::SμF*, *pTET-lys2::SμR* and *pTET-lys2::Cβ2* reporters under both low- and high-transcription conditions (Table 1). Upon loss of Sgs1 under low-transcription conditions, recombination rates were elevated by 1.5- to 5- fold, consistent with the hyper-recombination phenotype observed in other systems [36]. A further increase in the recombination rate for each construct was observed when transcription was activated in the *sgs1* background. Although not statistically significant, we note that the recombination rate for the *pTET-lys2::SμF* construct was 2-fold higher than the rates obtained with either the *pTET-lys2::SμR* or *pTET-lys2::Cβ2* reporters.

3.4. Increase in SμF-associated instability upon loss of RNase H and Sgs1

Because switch region-associated G-loops in *E. coli* have been detected in RecQ and RNase H-deficient, but not in WT cells [8], we examined the rates of Sμ-associated recombination in *sgs1 rnh1 rnh201* triple mutant yeast strains (Table 1). While the recombination rates for all three constructs were similar under low-transcription conditions, there was a striking difference under high-transcription conditions. The recombination rate for the *pTET-lys2::SμF* construct was 7.7-fold higher than that associated with the *pTET-lys2::SμR* reporter, and 5.6-fold higher than obtained with the *pTET-lys2::Cβ2* construct. The orientation-dependent effect of the Sμ region on recombination in the RNase H-deficient background thus appears to be enhanced upon additional loss of Sgs1.

3.5. Effect of Top1 topoisomerase on Sμ-associated recombination

Yeast Top1 is a Type IB topoisomerase that can relieve both positive and negative torsional stress in DNA [37]. It covalently attaches to the 3' end of DNA, creating a single strand nick, which is quickly religated after swiveling of the DNA strands to remove supercoiling. During highly activated transcription, positive and negative supercoiling can build up in front of or behind RNA polymerase complexes, respectively [38]. In absence of Top1, extensive R-loop formation and regions of DNA helix melting have been observed in the highly transcribed rDNA repeat locus [39, 40].

In order to determine the effect of accumulated torsional stress on the stability of G-run containing sequence, we examined the rates of Sμ-associated recombination in Top1-

deficient strains (Table 1). Under low transcription conditions, there were slight increases (less than 2-fold) in the recombination rates for the *pTET-lys2::SμF* and *pTET-lys2::Cβ2* constructs. When transcription was activated in the *top1* background, the recombination rates for the *pTET-lys2::SμR* and *pTET-lys2::Cβ2* constructs were elevated by ~4-fold. A more striking increase (25-fold) was observed for the recombination rate of the *pTET-lys2::SμF* construct in a *top1* background under high-transcription conditions. The resulting recombination rate for the *pTET-lys2::SμF* allele was 10- and 9- fold higher than the recombination rates for *pTET-lys2::SμR* or *pTET-lys2::Cβ2* constructs, respectively.

3.6. Effect of Pif1 helicase on Sμ-associated recombination

Given the role of Pif1 in maintaining stability of the human CEB1 minisatellite [16], we explored whether Pif1 is likewise important for limiting recombination associated with the *pTET-lys2::SμF*, *pTET-lys2::SμR* or *pTET-lys2::Cβ2* reporters (Table 2). Under low-transcription conditions, loss of Pif1 elevated *pTET-lys2::Cβ2* - associated recombination 45-fold, but increased *pTET-lys2::SμF*- and *pTET-lys2::SμR* - associated recombination only 8.5-fold. High levels of transcription in the *pif1* background stimulated recombination involving the *pTET-lys2::SμF* and *pTET-lys2::SμR* constructs approximately 4.5-fold, and had a slightly smaller effect (2.5-fold) on recombination associated with the *pTET-lys2::Cβ2* reporter. The stabilizing effect of Pif1 on recombination in our system thus does not appear to be related to the potential of GC-rich sequences to form co-transcriptional G4 DNA.

3.7. Effect of Mft1 loss on Sμ-associated recombination

THO is a multi-functional protein complex involved in mRNA processing and mRNP export, as well as in efficient elongation by the RNAP II holoenzyme (reviewed in [41]). Disabling the THO complex promotes R-loop formation and generally leads to a strong hyperrecombination phenotype [35, 42]. Mft1 is a component of the THO complex and deletion of the *MFT1* gene results in THO-defective, hyper-recombination phenotype [41]. In an *mft1* background under low-transcription conditions, we observed a large, ~40-fold increase in recombination rates for the *pTET-lys2::Sμ* constructs, but only a 16-fold increase for the *pTET-lys2::Cβ2* allele (Table 2). Although high-transcription further elevated recombination in the *mft1* background, the effect was greater with the *pTET-lys2::SμR* than with the *pTET-lys2::SμF* construct (3.1- and 1.5-fold increases, respectively). It should be noted that this is the reverse of the orientation-dependent effect observed in the *rnh1 rnh201* double mutant.

We also examined the effect of transcription on recombination in an *mft1 sgs1* double mutant background. Interestingly, Sgs1 loss had opposing effects under low-versus high-transcription conditions in the *mft1* background. Recombination rates were uniformly reduced in the *mft1 sgs1* double relative to the *mft1* single mutant under low-transcription conditions, but uniformly elevated under high-transcription conditions. We currently have no explanation for this difference. While transcription in the *mft1 sgs1* background stimulated recombination with all three substrates, the effect was again slightly greater for the *pTET-lys2::SμR* than for the *pTET-lys2::SμF* or *pTET-lys2::Cβ2* construct (29- versus 12-fold, respectively).

3.8. Effect of AID expression on Sμ-associated recombination rates

Activation-induced deaminase (AID) is a single-strand specific deaminase that converts cytosine to uracil [43] and is required for the somatic hypermutation (SHM) of immunoglobulin variable region genes as well as the heavy chain class switch recombination (CSR) [44]. Transcription is required for both SHM and CSR, and is thought to facilitate access of AID to single-stranded DNA. AID has previously been shown to stimulate recombination and mutagenesis in a transcription-dependent manner in THO-

defective yeast strains [45]. It was also recently shown that a defective THO complex together with AID expression enhances chromosomal translocations mediated by non-homologous end joining (NHEJ), presumably by inducing double-strand breaks in the murine $S\mu$ sequence [46]. In order to examine the effect of AID expression on homologous recombination, we ectopically expressed the human AID (hAID) in strains containing the *pTET-lys2::S μ* constructs. While there was no stimulation of recombination in a WT background with the *pTET-lys2::S μ F* construct, there was a 7-fold stimulation of recombination with the *pTET-lys2::S μ R* construct (Table 3). Deletion of the uracil DNA glycosylase gene (*UNG1*) eliminated the hAID-stimulated recombination observed with the *pTET-lys2::S μ R* construct, confirming that the elevated recombination occurs through the processing of uracil intermediates.

In an *mft1* mutant background where extensive R-loop formation was previously reported [35], expression of hAID was accompanied by a large stimulation of recombination for both constructs (Table 3). As in the WT background, however, hAID expression was associated with an orientation-dependent bias in the stimulation of recombination in the *mft1* background. With hAID expression, the recombination rate of *pTET-lys2::S μ R* construct was ~ 9-fold higher than that of the *pTET-lys2-S μ F* construct. In a *top1* background, hAID expression was associated with similar orientation bias (Table 3). While there was no stimulation of recombination of the *pTET-lys2-S μ F* construct, the rate of recombination for the *pTET-lys2::S μ R* construct was stimulated by ~ 16-fold with hAID expression.

4. Discussion

Homologous recombination is a high-fidelity repair process that is initiated by single-strand gaps or double-strand breaks in duplex DNA, and is a sensitive indicator of DNA damage. In the current study, a yeast recombination assay has been used to examine genetic instability associated with the repetitive mouse immunoglobulin $S\mu$ sequence, as well as with a control, nonrepetitive sequence ($C\beta 2$) of comparable size and GC content. Each test sequence was engineered into a full-length, chromosomal *LYS2* gene, which served as the recipient of genetic information provided by a truncated *lys2* allele on a different chromosome. According to standard models of recombination, the recipient allele is the site of the recombination-initiating lesion. By placing the $S\mu$ sequence in both directions within a *pTET*-regulated *LYS2* gene, we have also been able to discern orientation-specific effects of this sequence on mitotic recombination rates. The $S\mu$ sequence is in its physiological orientation in the *pTET-lys2::S μ F* allele, with the G-rich strand being the non-transcribed strand; the G-rich strand is the transcribed strand in the *pTET-lys2::S μ R* allele.

In the absence of highly activated transcription in a WT background, both $S\mu$ inserts were associated with a higher recombination rate than was the control $C\beta 2$ sequence. Given the similar sizes and GC contents of these sequences, and the further enhancement of $S\mu$ - $C\beta 2$ difference in an *mft1* background (see below), we suggest that this likely reflects the repetitive nature of the $S\mu$ sequence. When the transcription was turned on to a high level, the recombination rate associated with each construct increased a comparable amount (5-10 fold). Under high-transcription conditions in RNase H-defective background, however, there were many more recombinants generated with the *pTET-lys2::S μ F* allele than with the *pTET-lys2::S μ R* or *pTET-lys2::C $\beta 2$* allele. We suggest that the difference reflects more efficient formation and/or enhanced stability of co-transcriptional RNA:DNA hybrids (R-loops) with the *pTET-lys2::S μ F* allele. Increased R-loops could be due to the greater stability of RNA:DNA hybrids when the RNA strand is the purine-rich strand [47], enhanced nucleation of R-loop formation by clusters of guanines on the nascent transcript [48], and/or a stabilizing feature of the single strand of DNA excluded from the R-loop. With regard to the latter possibility, it should be noted that additional elimination of the

Sgs1 helicase further enhanced the orientation-dependent effect of S μ sequences on recombination. An intriguing possibility is that lack of RNase H in yeast provides greater opportunity for G4 DNA to form on the nontranscribed strand of the *pTET-lys2::S μ F* allele, and once formed, Sgs1 can unwind at least some of the G4 DNA. We suggest a situation analogous to that reported previously in *E. coli*, where a physiologically oriented murine S μ sequence forms co-transcriptional G-loops in cells deficient in RNase H and RecQ [8]. Finally, the recent demonstration that the S μ sequence efficiently blocks RNA polymerase when the G-rich sequence is present on the nontranscribed strand [49] suggests another possible contributor to the orientation-dependent instability of the S μ sequence in our system.

The absence of Top1 results in a build up of helical torsion in highly transcribed areas and, in *E. coli*, results in extensive R-loop formation that can be relieved by overexpression of RNase H [50]. In the highly transcribed rDNA locus in yeast, Top1 deficiency results in extensive formation of R-loops and “topo bubbles” which are regions of strand separation due to the accumulation of negative supercoils [39, 40]. Similar to the effect of RNase H deficiency, an orientation-specific increase in instability was observed with the highly transcribed *pTET-lys2::S μ* alleles in a *top1* background, with the *pTET-lys2::S μ F* allele generating 10-fold more recombinants than the *pTET-lys2::S μ R*. This difference can be explained by enhanced G4 DNA formation due to more extensive RNA-DNA hybrids on the transcribed strand and increased single-stranded character on the G-containing non-transcribed strand of the *pTET-lys2::S μ F* construct.

Another way to promote RNA:DNA hybrid formation is through disruption of the THO complex [35], which is important for processing nascent transcripts [41]. Unexpectedly, *mft1* mutants with a defective THO complex exhibited a recombination phenotype in our system that was distinct from that observed in the absence of RNase H activity or Top1. First, under low-transcription conditions in an *rnh1 rnh201* background, the S μ and C β 2 constructs were associated with similar recombination rates. By contrast, the C β 2-containing construct produced 7-fold fewer recombinants than either the S μ F or S μ R construct in an *mft1* mutant. Given the similar GC contents of the test sequences, the Mft1-related difference may reflect the role of the THO complex in promoting transcription through the repetitive S μ sequences [51]. Second, whereas there were 5 - 10-fold more recombinants obtained with the S μ F than with the S μ R construct under high-transcription conditions in either RNase H- or Top1-deficient background, there were 2-fold more recombinants with the S μ R than with the S μ F construct in the *mft1* mutant. A reason for this difference is not immediately obvious, but could reflect impaired transcription of S μ sequences that is unrelated to R-loop formation, or more global changes in gene expression in the absence of the THO complex.

The yeast Pif1 helicase can unwind G4 DNA *in vitro* and its absence greatly increases recombination-dependent instability associated with the human CEB1 minisatellite [16]. Given that S μ sequences also form G4 DNA *in vitro*, we anticipated that Pif1 loss would be associated with an orientation-dependent increase in S μ -associated recombination. Although recombination was elevated in the *pif1* background, the greater effect we expected to see with the *pTET-lys2::S μ F* than with the *pTET-lys2::S μ R* construct, especially under high-transcription conditions, was not observed. G4 DNA structures are known to vary depending on the primary sequence of the G-rich motifs [52], however, and it is possible that Pif1 is specific for the CEB1-associated structure. Alternatively, the disparity in the *pif1* results could reflect inherent differences in the two assay systems. In the CEB1 system, the assay measures the interstitial deletion within repeats where the repair template was presumably the sister chromatid [16]. In contrast, the repair template in our S μ system is on a nonhomologous chromosome. Also, the CEB1 sequence was embedded in a non-transcribed

region and the formation of the associated G4 DNA was attributed to the process of replication. In our system, highly activated transcription is necessary to reveal the difference in stability between G-loop forming ($S_{\mu}F$) and non-G-loop forming ($S_{\mu}R$) sequences and, thus, G4 formation is clearly co-transcriptional.

In addition to the potential of S_{μ} sequences to form non-B DNA structures, these sequences are also targets of AID, which exhibits single-strand specific cytosine deaminase activity *in vitro*. During CSR, the uracils generated by AID activity are excised by uracil DNA glycosylases and then are further processed by base excision repair enzymes to produce recombination-initiating breaks in DNA [29, 40]. The uneven distribution of G's and C's between the two strands of the S_{μ} fragment used here (the C-rich strand contains 358 cytosines but only 117 guanines) allowed us to infer whether AID more efficiently targets S_{μ} -associated cytosines when they are on the nontranscribed as opposed to the transcribed strand of a highly expressed gene. As predicted by its preference for single-stranded DNA, expression of hAID in yeast increased the recombination rate associated with the *pTET-lys2-S_μR* allele 7- and 16-fold in WT and *top1* backgrounds, respectively, but had no effect on recombination with the *pTET-lys2-S_μF* allele in either background. As seen in prior experiments [45], the effect of AID on recombination was greatly amplified in an *mft1* background. The heterologous expression of AID was recently reported to increase chromosomal translocations at both the physiologically and inversely oriented S_{μ} sequence fragments embedded in THO-deficient yeast strains [46]. Although the extent of instability observed by Ruiz *et al.* was higher for the physiologically oriented S_{μ} sequence, the reverse of the pattern reported here, this difference could reflect the larger size of the S_{μ} fragments used in our assays or basic differences between the two systems.

The genome-destabilizing potential of repeat-containing sequence motifs is closely linked to their ability to assume non-B DNA structures *in vivo*. Using yeast as a model system, we have demonstrated that mitotic instability associated with the murine S_{μ} sequence is increased by transcription and exhibits strong orientation dependence. Our data point to two possible factors that can promote G-loop formation – highly activated transcription and the associated accumulation of DNA superhelical stresses in the absence of Top1 (Figure 2). Once formed, RNase Hs function to destabilize G-loops by degradation of RNA, which is consistent with the formation of RNA:DNA hybrids and co-transcriptional G-loop structures. G-loops can also be destabilized by Sgs1 helicase, which presumably unwind G quartets on the non-transcribed strand. Although this system appears to recapitulate some physiological features associated with S_{μ} sequences, it is not intended to model the process of CSR. The assay system used here, however, will be useful in investigating whether the collision between transcription and replication machineries can influence the stability of G-loop forming sequences and also in elucidating additional helicases and nucleases that might function to collapse G-loop structures. The general approach outline in this study can also be used to study the requirements of maintaining other types of repetitive sequences that have been associated with genetic instability.

Acknowledgments

The authors thank F. Alt for the gift of pT7- S_{μ} , Y. Pavlov for pESC-LEU-hAIDsc, and T. Petes for the critical reading of the manuscript. This work was supported by NIH grant GM38464 to SJ-R.

References

- [1]. Bacolla A, Wojciechowska M, Kosmider B, Larson JE, Wells RD. The involvement of non-B DNA structures in gross chromosomal rearrangements. *DNA Repair (Amst)*. 2006; 5:1161–1170. [PubMed: 16807140]

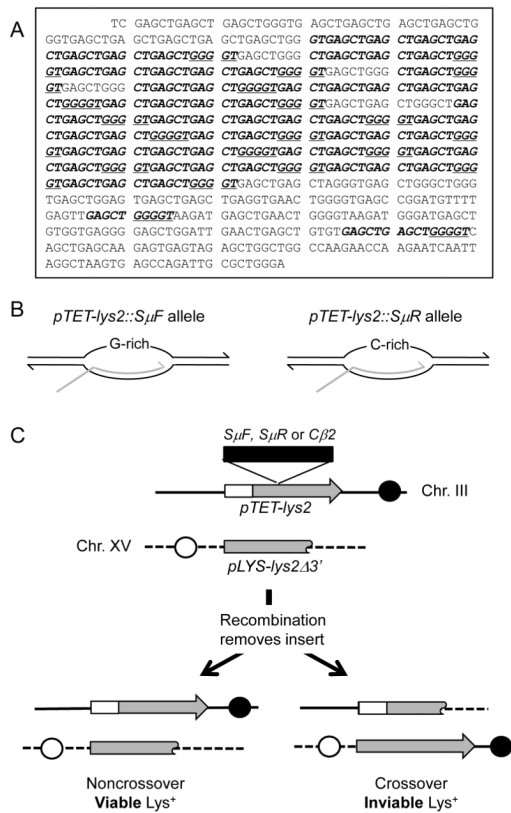
- [2]. Gordenin DA, Resnick MA. Yeast ARMs (DNA at-risk motifs) can reveal sources of genome instability. *Mutat Res.* 1998; 400:45–58. [PubMed: 9685581]
- [3]. Sen D, Gilbert W. Formation of parallel four-stranded complexes by guanine-rich motifs in DNA and its implications for meiosis. *Nature.* 1988; 334:364–366. [PubMed: 3393228]
- [4]. Maizels N. Dynamic roles for G4 DNA in the biology of eukaryotic cells. *Nat Struct Mol Biol.* 2006; 13:1055–1059. [PubMed: 17146462]
- [5]. Lipps HJ, Rhodes D. G-quadruplex structures: in vivo evidence and function. *Trends Cell Biol.* 2009; 19:414–422. [PubMed: 19589679]
- [6]. Duquette ML, Huber MD, Maizels N. G-rich proto-oncogenes are targeted for genomic instability in B-cell lymphomas. *Cancer Res.* 2007; 67:2586–2594. [PubMed: 17363577]
- [7]. Willis TG, Dyer MJ. The role of immunoglobulin translocations in the pathogenesis of B-cell malignancies. *Blood.* 2000; 96:808–822. [PubMed: 10910891]
- [8]. Duquette ML, Handa P, Vincent JA, Taylor AF, Maizels N. Intracellular transcription of G-rich DNAs induces formation of G-loops, novel structures containing G4 DNA. *Genes Dev.* 2004; 18:1618–1629. [PubMed: 15231739]
- [9]. Schawalder J, Paric E, Neff NF. Telomere and ribosomal DNA repeats are chromosomal targets of the bloom syndrome DNA helicase. *BMC Cell Biol.* 2003; 4:15. [PubMed: 14577841]
- [10]. Weitao T, Budd M, Campbell JL. Evidence that yeast *SGS1*, *DNA2*, *SRS2*, and *FOB1* interact to maintain rDNA stability. *Mutat Res.* 2003; 532:157–172. [PubMed: 14643435]
- [11]. Smith S, Banerjee S, Rilo R, Myung K. Dynamic regulation of single-stranded telomeres in *Saccharomyces cerevisiae*. *Genetics.* 2008; 178:693–701. [PubMed: 18245359]
- [12]. Stavropoulos DJ, Bradshaw PS, Li X, Pasic I, Truong K, Ikura M, Ungrin M, Meyn MS. The Bloom syndrome helicase BLM interacts with TRF2 in ALT cells and promotes telomeric DNA synthesis. *Hum Mol Genet.* 2002; 11:3135–3144. [PubMed: 12444098]
- [13]. Killen MW, Stults DM, Adachi N, Hanakahi L, Pierce AJ. Loss of Bloom syndrome protein destabilizes human gene cluster architecture. *Hum Mol Genet.* 2009; 18:3417–3428. [PubMed: 19542097]
- [14]. Sun H, Bennett RJ, Maizels N. The *Saccharomyces cerevisiae* Sgs1 helicase efficiently unwinds G-G paired DNAs. *Nucleic Acids Res.* 1999; 27:1978–1984. [PubMed: 10198430]
- [15]. Sun H, Karow JK, Hickson ID, Maizels N. The Bloom's syndrome helicase unwinds G4 DNA. *J Biol Chem.* 1998; 273:27587–27592. [PubMed: 9765292]
- [16]. Ribeyre C, Lopes J, Boule JB, Piazza A, Guedin A, Zakian VA, Mergny JL, Nicolas A. The yeast Pif1 helicase prevents genomic instability caused by G-quadruplex-forming CEB1 sequences in vivo. *PLoS Genet.* 2009; 5:e1000475. [PubMed: 19424434]
- [17]. Kruisselbrink E, Guryev V, Brouwer K, Pontier DB, Cuppen E, Tijsterman M. Mutagenic capacity of endogenous G4 DNA underlies genome instability in FANCI-defective *C. elegans*. *Curr Biol.* 2008; 18:900–905. [PubMed: 18538569]
- [18]. Sundararajan R, Gellon L, Zunder RM, Freudenreich CH. Double-strand break repair pathways protect against CAG/CTG repeat expansions, contractions and repeat-mediated chromosomal fragility in *Saccharomyces cerevisiae*. *Genetics.* 2010; 184:65–77. [PubMed: 19901069]
- [19]. Balakumaran BS, Freudenreich CH, Zakian VA. CGG/CCG repeats exhibit orientation-dependent instability and orientation-independent fragility in *Saccharomyces cerevisiae*. *Hum Mol Genet.* 2000; 9:93–100. [PubMed: 10587583]
- [20]. Kim HM, Narayanan V, Mieczkowski PA, Petes TD, Krasilnikova MM, Mirkin SM, Lobachev KS. Chromosome fragility at GAA tracts in yeast depends on repeat orientation and requires mismatch repair. *EMBO J.* 2008; 27:2896–2906. [PubMed: 18833189]
- [21]. Lobachev KS, Stenger JE, Kozyreva OG, Jurka J, Gordenin DA, Resnick MA. Inverted Alu repeats unstable in yeast are excluded from the human genome. *EMBO J.* 2000; 19:3822–3830. [PubMed: 10899135]
- [22]. Tian M, Alt FW. Transcription-induced cleavage of immunoglobulin switch regions by nucleotide excision repair nucleases in vitro. *J Biol Chem.* 2000; 275:24163–24172. [PubMed: 10811812]

- [23]. Sikorski RS, Hieter P. A system of shuttle vectors and yeast host strains designed for efficient manipulation of DNA in *Saccharomyces cerevisiae*. *Genetics*. 1989; 122:19–27. [PubMed: 2659436]
- [24]. Freedman JA, Jinks-Robertson S. Genetic requirements for spontaneous and transcription-stimulated mitotic recombination in *Saccharomyces cerevisiae*. *Genetics*. 2002; 162:15–27. [PubMed: 12242220]
- [25]. Brachmann CB, Davies A, Cost GJ, Caputo E, Li J, Hieter P, Boeke JD. Designer deletion strains derived from *Saccharomyces cerevisiae* S288C: a useful set of strains and plasmids for PCR-mediated gene disruption and other applications. *Yeast*. 1998; 14:115–132. [PubMed: 9483801]
- [26]. Mayorov VI, Rogozin IB, Adkison LR, Frahm C, Kunkel TA, Pavlov YI. Expression of human AID in yeast induces mutations in context similar to the context of somatic hypermutation at G-C pairs in immunoglobulin genes. *BMC Immunol*. 2005; 6:10. [PubMed: 15949042]
- [27]. Goldstein AL, McCusker JH. Three new dominant drug resistance cassettes for gene disruption in *Saccharomyces cerevisiae*. *Yeast*. 1999; 15:1541–1553. [PubMed: 10514571]
- [28]. Kim N, Abdulovic AL, Gealy R, Lippert MJ, Jinks-Robertson S. Transcription-associated mutagenesis in yeast is directly proportional to the level of gene expression and influenced by the direction of DNA replication. *DNA Repair (Amst)*. 2007; 6:1285–1296. [PubMed: 17398168]
- [29]. Gueldener U, Heinisch J, Koehler GJ, Voss D, Hegemann JH. A second set of loxP marker cassettes for Cre-mediated multiple gene knockouts in budding yeast. *Nucleic Acids Res*. 2002; 30:e23. [PubMed: 11884642]
- [30]. Spell RM, Jinks-Robertson S. Determination of mitotic recombination rates by fluctuation analysis in *Saccharomyces cerevisiae*. *Methods Mol Biol*. 2004; 262:3–12. [PubMed: 14769952]
- [31]. Honjo T, Kinoshita K, Muramatsu M. Molecular mechanism of class switch recombination: linkage with somatic hypermutation. *Annu Rev Immunol*. 2002; 20:165–196. [PubMed: 11861601]
- [32]. Belli G, Gari E, Aldea M, Herrero E. Functional analysis of yeast essential genes using a promoter-substitution cassette and the tetracycline-regulatable dual expression system. *Yeast*. 1998; 14:1127–1138. [PubMed: 9778798]
- [33]. Cerritelli SM, Crouch RJ. Ribonuclease H: the enzymes in eukaryotes. *FEBS J*. 2009; 276:1494–1505. [PubMed: 19228196]
- [34]. Arudchandran A, Cerritelli S, Narimatsu S, Itaya M, Shin DY, Shimada Y, Crouch RJ. The absence of ribonuclease H1 or H2 alters the sensitivity of *Saccharomyces cerevisiae* to hydroxyurea, caffeine and ethyl methanesulphonate: implications for roles of RNases H in DNA replication and repair. *Genes Cells*. 2000; 5:789–802. [PubMed: 11029655]
- [35]. Huertas P, Aguilera A. Cotranscriptionally formed DNA:RNA hybrids mediate transcription elongation impairment and transcription-associated recombination. *Mol Cell*. 2003; 12:711–721. [PubMed: 14527416]
- [36]. Hickson ID. RecQ helicases: caretakers of the genome. *Nat Rev Cancer*. 2003; 3:169–178. [PubMed: 12612652]
- [37]. Wang JC. Cellular roles of DNA topoisomerases: a molecular perspective. *Nat Rev Mol Cell Biol*. 2002; 3:430–440. [PubMed: 12042765]
- [38]. Liu LF, Wang JC. Supercoiling of the DNA template during transcription. *Proc Natl Acad Sci U S A*. 1987; 84:7024–7027. [PubMed: 2823250]
- [39]. El Hage A, French SL, Beyer AL, Tollervey D. Loss of Topoisomerase I leads to R-loop-mediated transcriptional blocks during ribosomal RNA synthesis. *Genes Dev*. 2010; 24:1546–1558. [PubMed: 20634320]
- [40]. French SL, Sikes ML, Hontz RD, Osheim YN, Lambert TE, El Hage A, Smith MM, Tollervey D, Smith JS, Beyer AL. Distinguishing the roles of Topoisomerases I and II in relief of transcription-induced torsional stress in yeast rRNA genes. *Mol Cell Biol*. 2011; 31:482–494. [PubMed: 21098118]
- [41]. Rondon AG, Jimeno S, Aguilera A. The interface between transcription and mRNP export: from THO to THSC/TREX-2. *Biochim Biophys Acta*. 2010; 1799:533–538. [PubMed: 20601280]
- [42]. Chavez S, Beilharz T, Rondon AG, Erdjument-Bromage H, Tempst P, Svejstrup JQ, Lithgow T, Aguilera A. A protein complex containing Tho2, Hpr1, Mft1 and a novel protein, Thp2, connects

- transcription elongation with mitotic recombination in *Saccharomyces cerevisiae*. *EMBO J.* 2000; 19:5824–5834. [PubMed: 11060033]
- [43]. Bransteitter R, Pham P, Scharff MD, Goodman MF. Activation-induced cytidine deaminase deaminates deoxycytidine on single-stranded DNA but requires the action of RNase. *Proc Natl Acad Sci U S A.* 2003; 100:4102–4107. [PubMed: 12651944]
- [44]. Muramatsu M, Kinoshita K, Fagarasan S, Yamada S, Shinkai Y, Honjo T. Class switch recombination and hypermutation require activation-induced cytidine deaminase (AID), a potential RNA editing enzyme. *Cell.* 2000; 102:553–563. [PubMed: 11007474]
- [45]. Gomez-Gonzalez B, Aguilera A. Activation-induced cytidine deaminase action is strongly stimulated by mutations of the THO complex. *Proc Natl Acad Sci U S A.* 2007; 104:8409–8414. [PubMed: 17488823]
- [46]. Ruiz JF, Gomez-Gonzalez B, Aguilera A. AID Induces Double-Strand Breaks at Immunoglobulin Switch Regions and c-MYC Causing Chromosomal Translocations in Yeast THO Mutants. *PLoS Genet.* 2011; 7:e1002009. [PubMed: 21383964]
- [47]. Roberts RW, Crothers DM. Stability and properties of double and triple helices: dramatic effects of RNA or DNA backbone composition. *Science.* 1992; 258:1463–1466. [PubMed: 1279808]
- [48]. Roy D, Yu K, Lieber MR. Mechanism of R-loop formation at immunoglobulin class switch sequences. *Mol Cell Biol.* 2008; 28:50–60. [PubMed: 17954560]
- [49]. Tornaletti S, Park-Snyder S, Hanawalt PC. G4-forming sequences in the non-transcribed DNA strand pose blocks to T7 RNA polymerase and mammalian RNA polymerase II. *J Biol Chem.* 2008; 283:12756–12762. [PubMed: 18292094]
- [50]. Drolet M, Phoenix P, Menzel R, Masse E, Liu LF, Crouch RJ. Overexpression of RNase H partially complements the growth defect of an *Escherichia coli* delta topA mutant: R-loop formation is a major problem in the absence of DNA topoisomerase I. *Proc Natl Acad Sci U S A.* 1995; 92:3526–3530. [PubMed: 7536935]
- [51]. Voynov V, Verstrepen KJ, Jansen A, Runner VM, Buratowski S, Fink GR. Genes with internal repeats require the THO complex for transcription. *Proc. Nat. Acad. Sci. USA.* 2006; 103:14423–14428. [PubMed: 16983072]
- [52]. Neidle S. The structures of quadruplex nucleic acids and their drug complexes. *Curr Opin Struct Biol.* 2009; 19:239–250. [PubMed: 19487118]

Highlights

- We have developed a yeast genetic assay system to analyze genomic instability conferred by the repetitive G-rich immunoglobulin switch Mu region (S_{μ}) sequence.
- Activated transcription of S_{μ} sequence embedded in yeast genome leads to orientation-specific instability with the higher instability being observed when G-rich strand is on the non-transcribed strand mimicking the physiological orientation.
- Under conditions in which extended R-loop formation likely occurs – in the absence of Top1 or the loss of RNase H and Sgs1 helicase – we observed further increase in the instability of S_{μ} sequence and greater orientation bias.

**Figure 1.**

System for monitoring $S\mu$ -associated recombination.

A. Sequence of the DpnI fragment of murine immunoglobulin $S\mu$ region inserted into the BglIII site of *LYS2* gene. Uninterrupted (GAGCT) n GGGGT repeat units are indicated in bold italics and 4G runs are underlined.

B. Transcription orientations in the *pTET-lys2-SμF* and *pTET-lys2-SμR* constructs. Transcription bubbles are illustrated with the gray line indicating nascent mRNA. The single-stranded, non-transcribed strand is G-rich in the *pTET-lys2-SμF* construct and C-rich in the *pTET-lys2-SμR*.

C. Chromosomal configurations of the recombination substrates (see Material and Methods for details). Black and white circles indicate the locations of centromeres relative to the *lys2* alleles on Chr. III and Chr. XV, respectively. Recombination initiated by a gap or break within *pTET-lys2* allele removes the insert to create a *LYS*⁺ *pTET-LYS2* allele. Removal of the insert by recombination associated with a crossover event result in unviable acentric and dicentric products.

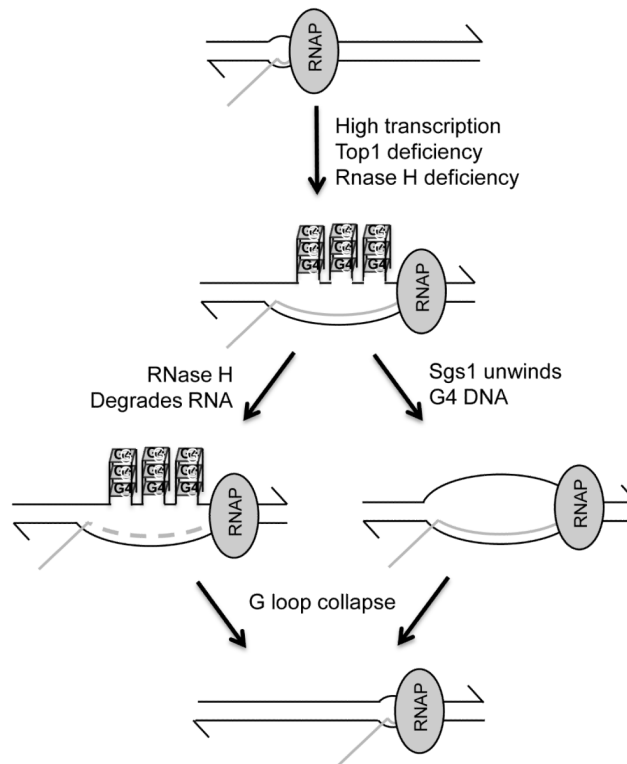


Figure 2.
Regulation of G-loop formation in highly transcribed DNA.
See Discussion for details.

Table 1Effect of RNase H, Sgs1 and Top1 on stability of S μ F, S μ R and C β 2 substrates

Allele	Genotype	Recombination rate $\times 10^{-8}$ (CI*)		
		Low transcription	High transcription	High/low
<i>lys2::SμF</i>	WT	2.94 (2.58 – 3.40)	20.3 (17.2 – 24.4)	6.9
	<i>rnh1 rnh201</i>	6.51 (3.88 – 10.4)	566 (289 – 780)	87
	<i>sgs1</i>	6.61 (4.73 – 12.6)	38.6 (29.6 – 49.7)	5.8
	<i>sgs1 rnh1 rnh201</i>	57.7 (46.7 – 66.8)	1500 (1190- 2480)	26
	<i>top1</i>	5.11 (4.54 – 5.68)	128 (113 – 177)	25
<i>lys2::SμR</i>	WT	2.70 (2.51 – 3.02)	12.5 (10.4 – 15.6)	4.6
	<i>rnh1 rnh201</i>	6.41 (4.92 – 9.76)	105 (78.8 – 135)	16
	<i>sgs1</i>	3.92 (3.46 – 6.11)	18.4 (15.4 – 32.7)	4.7
	<i>sgs1 rnh1 rnh201</i>	45.2 (33.0 – 47.0)	195 (163 – 251)	4.3
	<i>top1</i>	2.68 (2.24 – 3.05)	12.3 (10.3 – 18.1))	4.6
<i>lys2::Cβ2</i>	WT	1.01 (0.89 – 1.35)	8.55 (8.29 – 12.6)	8.4
	<i>rnh1 rnh201</i>	10.3 (8.26 – 16.9)	165 (134 – 215)	16
	<i>sgs1</i>	5.01 (3.71 – 10.3)	17.1 (15.7 – 21.7)	3.4
	<i>sgs1 rnh1 rnh201</i>	51.1 (24.4 – 54.9)	268 (204 – 344)	5.2
	<i>top1</i>	3.19 (2.62 – 3.43)	14.3 (12.2 – 18.4)	4.5

CI* - 95 % confidence interval.

Table 2Effects of Mft1 and Pif1 on stability of S μ F, S μ R and C β 2 substrates

Allele	Genotype	Recombination rate $\times 10^{-8}$ (CI*)	
		Low transcription	High transcription
<i>lys2::SμF</i>	WT	2.94 (2.58 – 3.40)	20.3 (17.2 – 24.4)
	<i>pif1</i>	24.9 (17.8 – 27.9)	107 (87 – 1640)
	<i>mft1</i>	124 (115 – 134)	181 (163 – 213)
	<i>mft1 sgs1</i>	24.2 (13.2 – 36.0)	320 (242 – 422)
<i>lys2::SμR</i>	WT	2.70 (2.51 – 3.02)	12.5 (10.4 – 15.6)
	<i>pif1</i>	23.3 (16.3 – 24.4)	111 (80 – 218)
	<i>mft1</i>	116 (86.1 – 124)	358 (309 – 410)
	<i>mft1 sgs1</i>	37.5 (34.4 – 61.9)	1070 (965 – 1590)
<i>lys2::Cβ2</i>	WT	1.01 (0.89 – 1.35)	8.55 (8.29 – 12.6)
	<i>pif1</i>	45.5 (33.0 – 75.1)	114 (88 – 157)
	<i>mft1</i>	16.3 (13.0 – 17.8)	67.3 (48.7 – 136)
	<i>mft1 sgs1</i>	10.0 (3.57 – 11.6)	124 (21.8 – 456)

CI* - 95 % confidence interval.

Table 3hAID and stability of S μ F and S μ R under high-transcription conditions

Genotype	Plasmid	Recombination rate $\times 10^{-8}$ (CI*)	
		<i>lys2::SμF</i>	<i>lys2::SμR</i>
WT	Empty vector	19.2 (17.4 – 27.8)	14.8 (12.8 – 17.0)
	Vector + hAID	20.9 (19.3 – 22.5)	102 (73.2 – 114)
<i>ung1</i>	Empty vector	21.8 (20.1 – 23.8)	11.7 (8.58 – 13.9)
	Vector + hAID	20.1 (19.2 – 22.3)	16.7 (10.6 – 21.6)
<i>mfi1</i>	Empty vector	89.7 (51.4 – 134)	359 (265 – 594)
	Vector + hAID	3020 (1190 – 5400)	26000 (19100 – 29200)
<i>top1</i>	Empty vector	138 (99.7 – 174)	18.0 (15.8 – 19.9)
	Vector + hAID	171 (123 – 293)	282 (253 – 294)

CI* - 95 % confidence interval.